personal" condition; the others were assigned to the "moral-impersonal" condition.
10. Participants were five male and four female undergraduates in Experiment 1, four male and five female in Experiment 2. All participants provided written informed consent.
11. Dilemmas were presented in random order in a series of six blocks of ten trials each in Experiment 1, twelve blocks of five trials each in Experiment 2. Participants' responses to versions of the trolley and footbridge dilemmas were consistent with the intuitions described above (*8*).
12. Stimuli (dilemmas) were presented on a visual display projected into the scanner. Each dilemma was presented as text through a series of three screens, the first two describing a scenario and the last posing a question about the appropriateness of an action one might perform in that scenario (e.g., turning the trolley). Participants were allowed to read at their own pace, pressing a button to advance from the first to the second screen and from the second to the third screen. After reading the third screen participants responded by pressing one of two buttons ("appropriate" or "inappropriate"). Participants were given a maximum of 46 s to read all three screens and respond. The intertrial interval (ITI) lasted for a minimum of 14 s (seven images) in each trial, allowing the hemodynamic response to return to baseline after each trial. Baseline activity was defined as the mean signal across the last four images of the ITI. Task-related activity was measured using a "floating window" of eight images surrounding (four before, one during, and three after) the point of response. (This window includes three post-response images in order to allow for the 4- to 6-s delay in hemodynamic response to neural activation.) This "floating window" technique combined the benefits of an event-related design with the flexibility required to image a complex and temporally extended psychological process that inevitably proceeds at its own pace. In Experiment 1, functional images were acquired in 20 axial slices parallel to the AC-PC (anterior commisure–posterior commisure) line [spiral pulse sequence; repetition time (TR), 2000 ms; echo time (TE), 45 ms; flip angle, 80°; field of view (FOV), 240 mm; 3.75-mm isotropic voxels] using a 1.5-T GE Signa whole-body scanner. In Experiment 2, functional images were acquired in 22 axial slices parallel to the AC-PC line (echoplanar pulse sequence; TR, 2000 ms; TE, 25 ms; flip angle, 90°; FOV, 192 mm; 3.0-mm isotropic voxels; 1-mm interslice spacing) using a 3.0-T Siemens Allegra head-dedicated scanner.
13. Before statistical analysis, images for all participants were coregistered using a 12-parameter automatic algorithm. Images were smoothed with an 8-mm full-width at half maximum (FWHM) 3D Gaussian filter. In Experiment 1, the images contained in each response window were analyzed with the use of a voxelwise mixed-effects ANOVA with participant as a random effect, and dilemma-type, block, and response-relative image as fixed effects. Statistical maps of voxelwise F-ratios were thresholded for significance ($P < 0.0005$) and cluster size (≥8 voxels). In Experiments 1 and 2, planned comparisons for significant differences between conditions ($P < 0.05$, cluster size ≥8 voxels) were made for each area identified by the thresholded ANOVA in Experiment 1.
14. R. J. Maddock, *Trends Neurosci.* **22**, 310 (1999).
15. S. M. Kosslyn *et al.*, *Neuroreport* **7**, 1569 (1996).
16. E. M. Reiman *et al.*, *Am. J. Psychiatry* **154**, 918 (1997).
17. W. C. Drevets, M. E. Raichle, *Cognition Emotion* **12**, 353 (1998).
18. E. E. Smith, J. Jonides, *Cognit. Psychol.* **33**, 5 (1997).
19. J. D. Cohen *et al.*, *Nature* **386**, 604 (1997).
20. In BA 7/40 (right) a small minority of voxels (10 of 91) showed a significant difference between the moral-impersonal and non-moral conditions.
21. Due to magnetic susceptibility artifact we were unable to image the orbitofrontal cortex, an area thought by some to play an important role in moral judgment (*3*).
22. Experiments 1 and 2 were not identical (*8*). Experiment 2 employed some modified versions of dilemmas from Experiment 1 as well as some new dilemmas in order to avoid a confound present in the design of the behavioral aspect of Experiment 1 (*24*).
23. The replicated results for BAs 9/10, 31, and bilateral 7/40 were achieved at a higher significance threshold in Experiment 2 ($P < 0.01$) than in Experiment 1.
24. A potential confound in the design of the behavioral aspect of the present study deserves attention. One might suppose that participants respond more slowly when giving an "unconventional" response, i.e., a response that differs from that of the majority. One might suppose further that the moral-personal condition makes greater use of dilemmas for which the emotionally incongruent response is also the unconventional response (as in judging that one may push the man off the footbridge in the footbridge dilemma), thus confounding emotional incongruity with unconventionality in participants' responses. Therefore, an effect that we attribute to emotional engagement may simply be an effect of the conventionality of participants' responses. To deconfound these factors, in Experiment 2 we included additional moral-personal dilemmas for which the conventional response was emotionally incongruent rather than congruent. For example, one dilemma asked whether it is appropriate to smother one's crying baby to death in order to prevent its crying from summoning enemy soldiers who will kill oneself, the baby, and a number of others if summoned. Most participants judged this action to be appropriate in spite of their putative emotional tendencies to the contrary. As predicted by our hypothesis, reaction times in such cases were significantly longer [t (8) = 4.332, $P < 0.0001$] than the reaction times for conventional and emotionally congruent responses, as were typically made in response to the footbridge dilemma. Thus, after controlling for conventionality, reaction times in the moral-personal condition are longer for trials which, according to our theory, reflect a judgment that is emotionally incongruent rather than congruent.
25. Although our conclusion concerning the behavioral influence of the observed emotional responses does not require that the emotion-related areas identified in Experiments 1 and 2 be different from areas that show increased activity in response to more basic kinds of emotional stimuli, one might wonder to what extent they do differ from such areas. We made a preliminary attempt to answer this question in the form of an addendum study to Experiment 1. Five participants responded to moral-personal and moral-impersonal dilemmas as in Experiments 1 and 2. Participants also performed a task in which they named the colors of visually presented emotional and neutral words, a task similar to the one used by Isenberg *et al.* (*27*). The emotional word stimuli were extracted from the text of the moral dilemmas by three independent coders. Neutral words and additional emotional words were drawn from materials used by Isenberg *et al.* (*27*). A comparison of the emotional and neutral word conditions (t test, $P < 0.05$, cluster size ≥8 voxels) revealed no significant activation in the emotion-related areas identified in Experiment 1 and only a marginal activation (9 out of 123 voxels) in one of the working memory areas (left BA 7/40). This comparison did, however, reveal activations in numerous other areas. A comparison of the moral-personal and moral-impersonal conditions from the same five sessions replicated the activations observed in Experiments 1 and 2 in BA 9/10 (55 of 64 voxels at $P < 0.05$) and left BA 7/40 (40 of 123 voxels at $P < 0.05$). These results demonstrate, at the very least, that the effects observed in Experiments 1 and 2 in the medial frontal gyrus (BA 9/10) cannot be attributed to the mere reading of emotional words. This area, more than any of the others we have identified, is likely to play a role in the integration of emotion and cognition in complex decision-making (*3*, *5*).
26. J. D. Haidt, *Psych. Rev.*, in press.
27. N. Isenberg *et al.*, *Proc. Natl. Acad. Sci. U.S.A.* **96**, 10456 (1999).
28. J. Talairach, P. Tournoux, *A Co-Planar Stereotaxic Atlas of the Human Brain* (Thieme, New York, 1988).
29. We gratefully acknowledge M. Gilzenrat, N. Isenberg, P. Jablonka, J. Kroger, and T.-Q. Li for their contributions to this project. Supported in part by grants from the Pew Charitable Trusts (no. 97001533-000) and the National Science Foundation (no. 2556566).

25 May 2001; accepted 30 July 2001

BAFF-R, a Newly Identified TNF Receptor That Specifically Interacts with BAFF

Jeffrey S. Thompson,[1] Sarah A. Bixler,[1] Fang Qian,[1] Kalpit Vora,[1]* Martin L. Scott,[1] Teresa G. Cachero,[1] Catherine Hession,[1] Pascal Schneider,[2] Irene D. Sizing,[1] Colleen Mullen,[1] Kathy Strauch,[1] Mohammad Zafari,[1] Christopher D. Benjamin,[1] Jurg Tschopp,[2] Jeffrey L. Browning,[1] Christine Ambrose[1]†

B cell homeostasis has been shown to critically depend on BAFF, the B cell activation factor from the tumor necrosis factor (TNF) family. Although BAFF is already known to bind two receptors, BCMA and TACI, we have identified a third receptor for BAFF that we have termed BAFF-R. BAFF-R binding appears to be highly specific for BAFF, suggesting a unique role for this ligand-receptor interaction. Consistent with this, the BAFF-R locus is disrupted in A/WySnJ mice, which display a B cell phenotype qualitatively similar to that of the BAFF-deficient mice. Thus, BAFF-R appears to be the principal receptor for BAFF-mediated mature B cell survival.

The TNF family ligand BAFF, also known as TALL-1, THANK, BLyS, and zTNF4 (*1*–*5*), enhances B cell survival in vitro (*6*) and has recently emerged as a key regulator of peripheral B cell populations in vivo. Mice overexpressing BAFF display mature B cell hyperplasia and symptoms of systemic lupus erythaematosus (SLE) (*7*). Likewise, some SLE patients have significantly increased levels of BAFF in their

serum (*8*). It has, therefore, been proposed that abnormally high levels of this ligand may contribute to the pathogenesis of autoimmune diseases by enhancing the survival of autoreactive B cells (*6*).

BAFF, a type II membrane protein, is produced by cells of myeloid origin (*1*, *4*) and is expressed either on the cell surface or in a soluble form (*1*). Two TNF receptor family members, BCMA and TACI, have been shown to interact with BAFF (*5*, *9*–*13*). APRIL, a TNF ligand with sequence homology to BAFF (*14*), also binds to these two receptors (*11*, *13*, *15*).

Initial studies using the BJAB B cell line suggested the existence of a third BAFF receptor: the cells bound high levels of BAFF, but surface BCMA was not detected and mRNA levels for TACI were low. Screening a BJAB expression library with BAFF yielded a cDNA (*16*) encoding a previously unknown 184–amino acid transmembrane protein that we have named BAFF-R (Fig. 1). The human BAFF-R gene was localized to chromosome 22q13.1-13.31 by homology to a bacterial artificial chromosome (BAC) clone (GenBank Z99716). BAFF-R is a type III transmembrane protein, like BCMA (*17*) and TACI (*18*). BAFF-R contains only four cysteine residues in its extracellular or ligand binding domain, making it the smallest cysteine-rich domain (CRD) in the TNF receptor family. TNF receptors are typically organized into multiple CRDs, each composed of six cysteine residues and three disulfide bonds (*19*). Distinct structural modules within the CRDs have been described (*20*). The spacing of the four cysteines in BAFF-R most closely resembles the C2 module found in BCMA, TACI, and TNFR (*17*). A murine BAFF-R cDNA was isolated from a B cell lymphoma library (*16*), and the encoded protein was found to be 56% identical to the human sequence, with the cysteine residues conserved in number and spacing (Fig. 1). The highest level of homology is in the COOH-terminal region of the proteins, where the sequence identity over 25 consecutive amino acids suggests a conserved signaling motif. BCMA also has some homology to BAFF-R in this region (*16*).

Northern blot analysis on human tissues revealed that BAFF-R is expressed as a 4.5-kb mRNA in the secondary lymphoid organs. High levels of BAFF-R mRNA were detected in the spleen and lymph nodes, lower levels were detected in the peripheral blood leukocytes and thymus, and none was detected in the bone marrow or fetal liver (Fig. 2, A and B). Similarly, murine BAFF-R was expressed at high levels in the spleen and at low levels in the lung and thymus (Fig. 2C). The murine BAFF-R mRNA is approximately 1.9 kb—significantly shorter than the human BAFF-R mRNA.

We determined that BAFF-R specifically bound BAFF with an affinity capable of blocking its function in vitro. When the isolated BAFF-R cDNA was transfected into cells, an antibody to human BAFF-R (anti-hBAFF-R) readily detected surface BAFF-R expression (Fig. 3A). A similar profile was obtained when BAFF was bound to these cells (Fig. 3A). Of note, BAFF bound to BAFF-R– and TACI-transfected cells with similar affinities (*16*). Further, BAFF binding to various B cell lines correlated strongly with the surface expression of BAFF-R, less so with TACI, and not at all with BCMA expression (*16*). Because several TNF family receptors have been shown to interact with more than one ligand (*21*), we tested the ability of 21 TNF ligands to bind to the extracellular domain of BAFF-R. Using BAFF-R:Fc fusion protein [the extracellular domain of BAFF-R fused to the Fc domain of human immunoglobulin G1 (hIgG1)], we found that human BAFF-R interacted with human and murine BAFF but did not bind to any other TNF ligand (Fig. 3B) (*22*). Most important, APRIL did not bind to BAFF-R:Fc, but it was shown to specifically bind to the TACI and BCMA fusion proteins (Fig. 3B). The functional importance of the BAFF–BAFF-R interaction was established when BAFF-R:Fc was used to block B cell proliferation and BAFF binding assays. Similar to BCMA:Fc, BAFF-R:Fc was able to completely inhibit BAFF-mediated co-stimulation of B cell proliferation (*1*, *4*) at a concentration of 10 μg/ml (Fig. 3C) (*23*). It also effectively blocked BAFF binding to the BJAB cell line (*16*).

A functional role of BAFF-R in the BAFF pathway was next examined with the use of A/WySnJ mice. The phenotype of this well studied mutant mouse line closely resembles that of BAFF knockout mice (*24*–*27*). In both

[1]Biogen, 12 Cambridge Center, Cambridge, MA 02142, USA. [2]The Institute of Biochemistry, University of Lausanne, CH-1066, Epalinges, Switzerland.

*Present address: Department of Biologics Research, Merck & Co., 126 East Lincoln Avenue, RY 80Y-310, Rahway, NJ 07065, USA.

†To whom correspondence should be addressed. E-mail: christine_ambrose@biogen.com

```
hBAFF-R   1    MRR-GPRSLRGRDAPAPTPCVPAECFDLLVRHCVACGLLRTPRPKPAGASSPAPRTAL
                 ||   || |:||: :|| |  :|||| |||:||:| |::||    : :||  | |||
mBAFF-R   1    MGARRLRVRSQRSRDSSVPTQCNQTECFDPLVRNCVSCELFHTP--DTGHTSSLEPGTAL

hBAFF-R  58    QPQESVGAGAGEAALPLPGLLFGAPALLGLALVLALV-LVGLVSWRRRQRRLRGASSAEA
               ||||      | |  |  :|| |||||||| |:|:|| ||:||||| ||: || ||
mBAFF-R  59    QPQE------GSALRPDVALLVGAPALLGLILALTLVGLVSLVSWRWRQQ-LRTAS----

hBAFF-R 117    PDGDKDAP-EPLDKVIILSPGISDATAPAWPPPGEDPGTTPPGHSVPVPATELGSTELVT
               || :: :  | |::|:: |     |:||:|||  ||  :: | ||||||||||||||||
mBAFF-R 108    PDTSEGVQQESLENVFVPSSETPHASAPTWPPLKEDADSALPRHSVPVPATELGSTELVT

hBAFF-R 176    TKTAGPEQQ
               ||||||||
mBAFF-R 168    TKTAGPEQ
```

Fig. 1. Aligned amino acid sequences of human and murine BAFF-R. Cysteine residues are in bold; the predicted transmembrane domain is underlined. The vertical lines indicate identical residues, and the dots, similar residues. The GenBank accession numbers are AF373846 for human BAFF-R and AF373847 for murine BAFF-R.

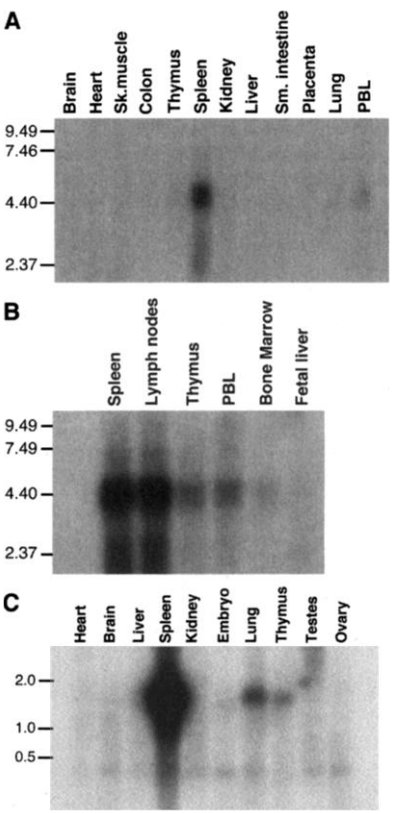

Fig. 2. Expression analysis of BAFF-R. Northern blot analysis of human BAFF-R is shown for (**A**) human multi-tissue blot and (**B**) immune system II blot (Clontech, Palo Alto, California). The filters were hybridized at 68°C with the use of a ^{32}P labeled Eco NI fragment from the BAFF-R cDNA in ExpressHyb buffer (Clontech). Filters were washed per manufacturer's protocol (Clontech) and exposed to film for 4 days. (**C**) A mouse tissue Northern blot (Ambion, Austin, Texas) was probed with the use of a labeled fragment from the mBAFF-R cDNA (excised with Pst I and Bgl I). The blot was hybridized, washed as above, and exposed for 1 day. An actin probe revealed similar mRNA levels in each lane.

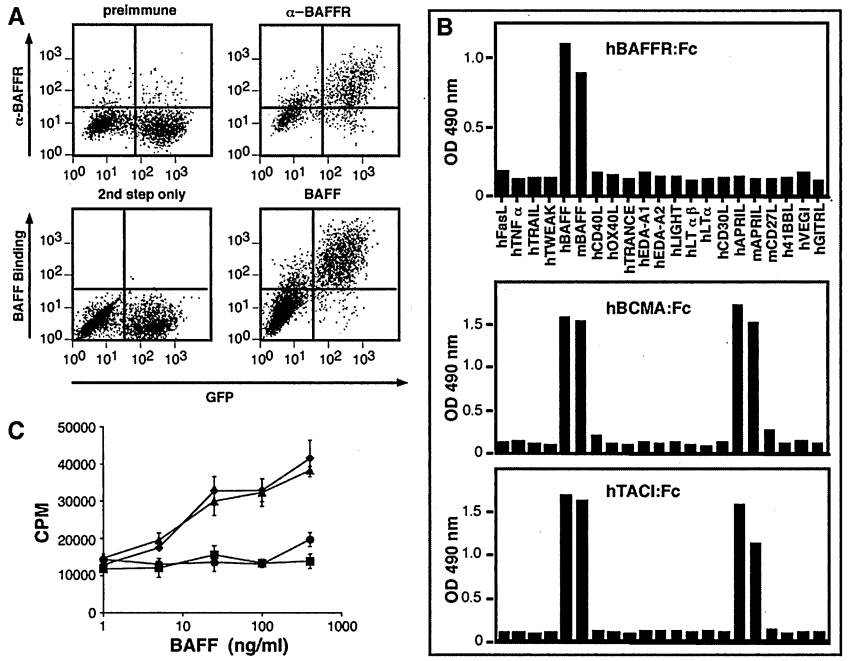

Fig. 3. Specific binding of BAFF to BAFF-R and inhibition with the use of BAFF-R:Fc. (**A**) BAFF-R is detected on the surface of 293E cells co-transfected with green fluorescence protein (GFP). Cells were stained with 1:100 dilution of preimmune sera or anti-BAFF-R peptide (aa 2–18) antibody (Rb 97) and detected with PE-conjugated antibody to rabbit IgG (Jackson ImmunoResearch). BAFF-R transfected cells were also stained with either no protein or biotinylated BAFF (1 μg/ml) and were detected with PE-streptavidin. (**B**) A panel of Flag-tagged TNF ligands was bound to BAFF-R:Fc, BCMA:Fc, or TACI:Fc coated plates and detected with the use of the HRP-M2 (Sigma). (**C**) The ability of BAFF-R:Fc (■), BCMA:Fc (●) or control IgG (▲) to block an in vitro co-stimulation assay is shown. BAFF plus antibody to IgM alone (◆). When various amounts of BAFF-R:Fc, BCMA:Fc or TACI:Fc were titrated into the proliferation assay, all the receptors showed half-maximal blocking around 250 ng/ml (*35*).

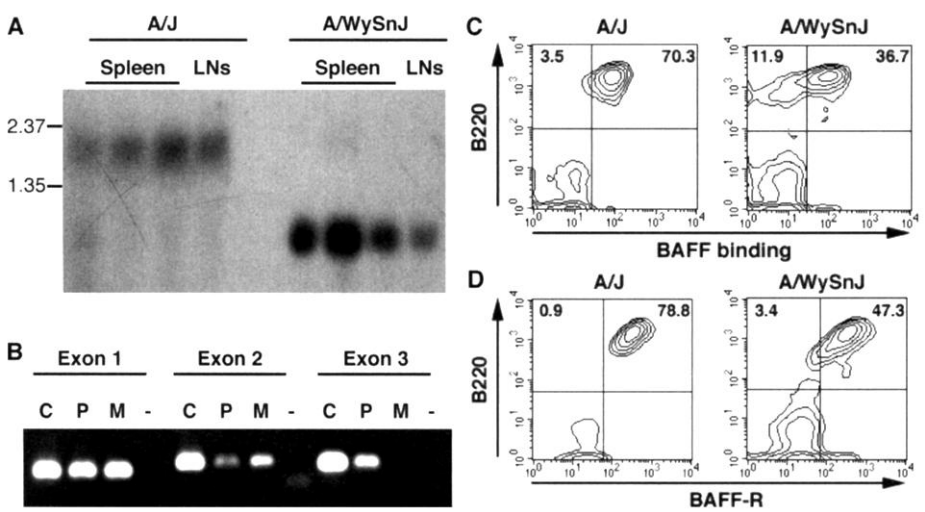

Fig. 4. Analysis of the A/WySnJ BAFF-R gene. (**A**) Northern blot analysis of spleen or lymph node RNA isolated from the A/J or A/WySnJ mouse lines (The Jackson Laboratory). Spleen RNA represents three different mice; the lymph node RNA was prepared from pooled tissue. Twenty micrograms of RNA was electrophoresed on a 1.2% formaldehyde gel. The gel was blotted and probed with a ^{32}P-labeled murine BAFF-R cDNA fragment. The filter was hybridized and washed as in Fig. 2. (**B**) PCR analysis of the BAFF-R coding region from A/J (P), A/WySnJ (M) genomic DNA, or a cloned mBAFF-R genomic fragment (C). Shown are the results of exon 1 (aa 1–48), exon 2 (aa 49–116), and exon 3 (aa 117–175) reactions. (**C**) FACS plot showing A/J or A/WySnJ splenocytes stained with APC-conjugated anti-B220 and biotinylated BAFF (200 ng/ml) followed by phycoerythrin (PE)-conjugated streptavidin (lymphocyte gate). (**D**) FACS analysis on splenocytes stained with APC-conjugated anti-B220 and a 1:2000 dilution of antibody to murine BAFF-R (Rb 116) followed by PE-conjugated donkey antibody to rabbit Ig.

mouse lines, the number of mature peripheral B cells is significantly reduced, although bone marrow B lymphopoiesis and peritoneal B1 cells are intact (*28*). The genomic defect in the A/WySnJ mice was recently localized to chromosome 15 between 27 and 56 centimorgan (*29*). We localized the murine BAFF-R gene to this region, approximately 48 cM on chromosome 15, by synteny with the use of sequence information from the human BAC that contains BAFF-R (*30*). The chromosomal location of the BAFF-R gene and the phenotype of A/WySnJ mice prompted us to look for a mutation in the A/WySnJ BAFF-R gene. Northern blot analysis on spleen and lymph node RNA from homozygous A/WySnJ mice and A/J parental mice indicated that the A/WySnJ BAFF-R mRNA was significantly shorter than the parental mRNA (Fig. 4A). Polymerase chain reaction (PCR) analysis of the A/WySnJ genomic DNA failed to detect an intact exon 3, which encodes the intracellular signaling domain of the protein (Fig. 4B) (*31*). The results of restriction enzyme analysis on the parental and mutant genomic DNA were not consistent with simple exon 3 deletion but rather with a more complex event(s) that could involve insertion, duplication, or rearrangement (*16*).

The disruption of the intracellular domain of the A/WySnJ BAFF-R protein does not eliminate expression of the extracellular and transmembrane domains located on exons 1 and 2. Fluorescence-activated cell sorting (FACS) analysis of A/WySnJ splenocytes stained with either an antibody to BAFF-R or with biotinylated BAFF revealed that surface BAFF-R was present and capable of binding BAFF, though the profiles were qualitatively and quantitatively different from wild-type B cells (Fig. 4, C and D) (*32*). Although the complete characterization of the A/WySnJ mutation will require further cloning and sequence analysis, the reduced number of mature B cells observed in these mice most likely results from the inability of the intracellular domain to engage in normal signal transduction.

The A/WySnJ mice exhibit a B cell phenotype similar, but not identical, to animals deficient in BAFF (*28*). Because the A/WySnJ mice do not have a complete null mutation, it is possible that some signaling occurs through BAFF-R or that TACI and/or BCMA compensate for the BAFF-R receptor defect, leading to a less severe phenotype than the BAFF knockout mice. In contrast, the B cell phenotypes of the BCMA- and TACI-deficient mice differ markedly from that observed in the BAFF-deficient mice (*28*, *33*, *34*). Antibody responses to various antigens have also been studied in these mice. BAFF-deficient mice are impaired for both T cell–dependent and –independent responses

(*28*), whereas A/WySnJ mice have normal T cell–independent responses, but impaired T cell–dependent responses (*25*) and TACI knockout mice are only deficient in the T-independent response (*34*).

We have identified BAFF-R, a previously unknown receptor specific for BAFF that has a role in BAFF signaling which is distinct from the two other known receptors for BAFF, BCMA, and TACI. A functional role for BCMA has not yet been defined, and even though TACI may play a role in T cell–independent responses, BAFF-R appears to be the principal receptor required for BAFF-mediated mature B cell survival and for generating an effective T cell–dependent immune response. Future studies on BAFF-R will more precisely elucidate its role in BAFF signaling.

References and Notes

1. P. Schneider *et al.*, *J. Exp. Med.* **189**, 1747 (1999).
2. H.-B. Shu, W.-H. Hu, H. Johnson, *J. Leukoc. Biol.* **65**, 680 (1999).
3. A. Mukhopadhyay, J. Ni, Y. Zhai, G.-L. Yu, B. B. Aggarwal, *J. Biol. Chem.* **274**, 15978 (1999).
4. P. A. Moore *et al.*, *Science* **285**, 260 (1999).
5. J. A. Gross *et al.*, *Nature* **404**, 995 (2000).
6. M. Batten *et al.*, *J. Exp. Med.* **192**, 1453 (2000).
7. F. Mackay *et al.*, *J. Exp. Med.* **190**, 1697 (1999).
8. J. Zhang *et al.*, *J. Immunol.* **166**, 6 (2001).
9. J. S. Thompson *et al.*, *J. Exp. Med.* **192**, 129 (2000).
10. X. Z. Xia *et al.*, *J. Exp. Med.* **192**, 137 (2000).
11. S. A. Marsters *et al.*, *Curr. Biol.* **10**, 785 (2000).
12. H. B. Shu, H. Johnson, *Proc. Natl. Acad. Sci. U.S.A.* **97**, 9156 (2000).
13. Y. Wu *et al.*, *J. Biol. Chem.* **275**, 35478 (2000).
14. M. Hahne *et al.*, *J. Exp. Med.* **188**, 1185 (1998).
15. P. Rennert *et al.*, *J. Exp. Med.* **192**, 1677 (2000).
16. Web figures 1 through 4, supplemental text (methods), and Web table 1 are available at *Science* Online at www.sciencemag.org/cgi/content/full/1061965/DC1.
17. C. Madry *et al.*, *Int. Immunol.* **10**, 1693 (1998).
18. G. U. von Bulow, R. J. Bram, *Science* **278**, 138 (1997).
19. C. A. Smith, T. Farrah, R. G. Goodwin, *Cell* **76**, 959 (1994).
20. J. H. Naismith, S. R. Sprang, *Trends Biochem. Sci.* **23**, 74 (1998).
21. R. M. Locksley, N. Killeen, M. J. Lenardo, *Cell* **104**, 487 (2001).
22. An enzyme-linked immunosorbent assay (ELISA) plate was coated with 5 μg/ml mouse anti-hIgG in carbonate buffer and then blocked (phosphate-buffered saline, 0.5% Tween-20, 4% nonfat milk). Twenty microliters of supernatant from receptor:Fc–transfected cells expressed in Optimem (Invitrogen, Carlsbad, CA) (about 1 to 10 μg/ml) was added to the plate. Purified protein was used for BAFF-R:Fc (20 μl at 2.7 μg/ml). The BAFF-R:Fc expression construct [amino acids 2 to 71 (aa 2–71)] was generated and protein produced similar to BCMA:Fc (*6*). Incubation with 20 μl of supernatant containing the Flag-tagged TNF ligands followed (*9*), and, after washing, the plates were incubated with 100 μl of M2-biotin (0.5 μg/ml) (Sigma, St. Louis, MO). Then, the plate was washed, incubated with 100-μl horseradish peroxidase (HRP)–streptavidin (1:4000; Jackson ImmunoResearch, West Grove, PA), washed, incubated with o-phenylenediamine (OPD) (Sigma) and read at 490 nm.
23. B cells were isolated from the spleens of C57BL/6 mice (8 weeks old; The Jackson Laboratory, Bar Harbor, ME) with the use of a B cell recovery column (Cedarlane Laboratories, LTD, Hornby, Ontario, Canada). Cells were incubated in 96-well plates [10^5 cells/well in 50 μl RPMI supplemented with 10% fetal bovine serum (FBS)] for 72 hours in the presence of various concentrations of human BAFF, 2 μg/ml of a goat antibody to human μ chain (Fab'2) (Jackson ImmunoResearch), and either no Ig or with control hIgG (10 μg/ml); purified human BAFF-R:Fc; or BCMA:Fc (aa 1–51) (10 μg/ml) (*9*). Cells were pulsed for 18 hours with [^{3}H]thymidine (1 μCi/well) and harvested. Incorporation was monitored by liquid scintillation counting.
24. D. J. Miller, C. E. Hayes, *Eur. J. Immunol.* **21**, 1123 (1991).
25. D. J. Miller, K. D. Hanson, J. A. Carman, C. E. Hayes, *Eur. J. Immunol.* **22**, 373 (1992).
26. V. M. Lentz, M. P. Cancro, F. E. Nashold, C. E. Hayes, *J. Immunol.* **157**, 598 (1996).
27. V. M. Lentz, C. E. Hayes, M. P. Cancro, *J. Immunol.* **160**, 3743 (1998).
28. B. Schiemann *et al.*, *Science* **294**, 2111 (2001).
29. K. A. Haog *et al.*, *Immunogenetics* **51**, 924 (2000).
30. X. Hua, J. Wu, J. L. Goldstein, M. S. Brown, H. H. Hobbs, *Genomics* **25**, 667 (1995).
31. Genomic DNA from A/J or A/WySnJ mice was prepared (*28*). A cloned Eco RI fragment containing the murine BAFF-R gene was used as a control. Either 10 ng of the cloned fragment or 100 ng of genomic DNA were used for PCR with *Pfu* buffer (Stratagene, La Jolla, CA), 10% dimethyl sulfoxide (DMSO), 0.2 mM deoxynucleoside triphosphates (dNTPs), 150 ng of each primer, and 1.25 units *Pfu* Turbo polymerase (Stratagene) and then cycled 30 times at 94°C for 30 s, 55°C for 1 min, and 72°C for 2 min. Primers are as follows: Exon 1, AAAGCGGCCGCCATG GGCGCCAGGAGACTCCG and GTCCAGTGTCCGGCGTGTGGA; Exon 2, GCAGCCTGGAGCCTGGGACAG and GGACTCCTTCTGAAG TGTCTG; Exon 3, GGAAAATGTCTTTGTACCCTC and AAAGCGG CCGCCTATTGCTCT GGGCCAGCTGT.
32. Splenocytes from 6- to 7-week-old A/J and A/WySnJ male mice were prepared by disruption of spleens between glass slides in Hanks' balanced salt solution (HBSS) plus 2% FBS that were strained through 70 μM nylon mesh and depleted of red blood cells (RBCs) by ammonium chloride lysis. After washing, cells were resuspended at 2 to 5 × 10^7 cells/ml in HBSS-FBS plus Fc block (10 μg/ml) (BD PharMingen, San Diego, CA). Cells were stained with biotinylated BAFF (200 ng/ml), anti-murine BAFF-R peptide (aa 139–154) or preimmune serum at a final dilution of 1:2000 for a period of 30 min. CyC-conjugated anti-CD3e and antigen-presenting cell (APC)–conjugated anti-B220 (PharMingen) were included in all staining reactions. After washing the cells, phycoerythrin (PE)–conjugated streptavidin (PharMingen) or PE-conjugated donkey anti-rabbit Ig (Jackson ImmunoResearch) were added for detection. Panels show scatter-gated cells (FACScalibur, Becton Dickinson, San Jose, CA). Data from 10,000 B220-positive cells are shown.
33. S. Xu, K.-P. Lam, *Mol. Cell Bio.* **21**, 4067 (2001).
34. G. U. von Bulow, J. M. van Deursen, R. J. Bram, *Immunity* **14**, 573 (2001).
35. F. Qian, T. Cachero, unpublished data.

36. We thank S. Kalled, Y.-M. Hsu and J. Naismith for helpful discussions. We are grateful to the DNA sequencing and analytical protein groups at Biogen, S. Mohan, A. Szilvasi, and S. Shulga-Morskaya for technical assistance, G. Thill, E. Garber, G. Farrington, and N. Horikoshi (Beth Israel Deaconess Medical Center, Boston) for reagents.

25 April 2000; accepted 27 July 2001
Published online 16 August 2001;
10.1126/science.1061965
Include this information when citing this paper.

An Essential Role for BAFF in the Normal Development of B Cells Through a BCMA-Independent Pathway

Barbara Schiemann,* Jennifer L. Gommerman, Kalpit Vora, Teresa G. Cachero, Svetlana Shulga-Morskaya, Max Dobles, Erica Frew, Martin L. Scott†

The B cell activating factor BAFF (BlyS/TALL-1/zTNF4) is a tumor necrosis factor (TNF)–related ligand that promotes B cell survival and binds to three receptors (BCMA, TACI, and the recently described BAFF-R). Here we report an absolute requirement for BAFF in normal B cell development. Examination of secondary lymphoid organs from BAFF-deficient mice revealed an almost complete loss of follicular and marginal zone B lymphocytes. In contrast, mice lacking BCMA had normal-appearing B lymphocyte compartments. BAFF therefore plays a crucial role in B cell development and can function through receptors other than BCMA.

B cell development is a temporally and spatially regulated process that begins in the bone marrow, where common lymphoid progenitors differentiate into pro–B cells, pre–B cells, and later, B lymphocytes (*1*, *2*). After B cell receptor expression, rearrangement, and deletion of autoreactive clones (*3*, *4*), a fraction of the cells migrate to secondary lymphoid organs. There, they may encounter antigen and undergo clonal selection and deletion in a complex series of steps (*5*, *6*). In the spleen, newly formed ($B220^+$, IgM^{hi}) cells acquire more mature phenotypes with down-regulation of IgM and up-regulation of molecules including CD21, CD23, and IgD.

A new TNF ligand thought to play a

Biogen, 14 Cambridge Center, Cambridge, MA 02142, USA.

*Present address: National Jewish Medical and Research Center, 1400 Jackson Street, Denver, CO 80206, USA.

†To whom correspondence should be addressed. E-mail: martin_scott@biogen.com